Int J Adv Manuf Technol (2014) 71:69–80
DOI 10.1007/s00170-013-5456-1

ORIGINAL ARTICLE

Evolutionary forging preform design optimization using strain-based criterion

Yong Shao · Bin Lu · Hengan Ou · Facai Ren · Jun Chen

Received: 4 May 2013 / Accepted: 24 October 2013 / Published online: 20 November 2013

Abstract Preform design plays an important role in forging design especially for parts with complex shapes. In this paper, an attempt was made to develop a topological optimization approach for the preform design in bulk metal forming processes based on the bidirectional evolutionary structural optimization strategy. In this approach, a new strain-based element addition and removal criterion has been proposed for evaluating and optimizing the material flow in the forging process. To obtain a smooth preform boundary, a closed B-spline curve based on the least square algorithm is employed to approximate the uneven surface of the updated preform profile. A C# program has been developed to integrate the FE simulation, shape optimization, and surface approximation processes. Two 2D forging preform design problems are evaluated by using the developed method. The results suggest that the optimized preform with the strain uniformity criterion has shown better performance in improving the material flow and deformation uniformity during the forging process. The results also demonstrate the robustness and efficiency of the developed preform optimization method.

Keywords Preform design · Optimization · Topology · Hot forging · Finite element

Y. Shao · B. Lu (✉) · F. Ren · J. Chen
National Die and Mold CAD Engineering Research Center, Shanghai Jiao Tong University, Shanghai 200030, China
e-mail: binlu@sjtu.edu.cn

Y. Shao
Jiangsu Provincial Key Laboratory of Advanced Welding Technology, Jiangsu University of Science and Technology, Zhenjiang 212003, China

H. Ou
Department of Mechanical, Materials and Manufacturing Engineering, University of Nottingham, Nottingham NG7 2RD, UK

1 Introduction

Formed parts with desired dimensional accuracy, satisfactory mechanical properties, as well as reduced cost are always in the pursuit of modern forging production. To achieve these objectives, multistage forging processes are often required to ensure proper material flow and distribution as well as minimum raw material consumption. In multistage forging processes, preform design plays an important role as a middle stage between the initial billet and the final forged shape. A proper preform design not only improves the material flow, final geometrical accuracy, and mechanical properties, but also reduces the forging load and die wear. Therefore, in-depth investigations on preform design and development of new optimization methods still offer significant potentials in the bulk metal forging process.

Traditional preform design is normally conducted by the trial-and-error approach requiring considerable number of forging trials, which is strongly dependent on designer's knowledge [1]. To obtain a proper preform design, a series of intelligent and programmed preform design methods combined with optimization theories have been developed based on numerical simulations recently. One earlier approach is the electric field theory. This approach employed the equipotential lines in the electric field to find out the preform shape, which was conducted only for the 2D preform design problems [2]. In recent years, 3D electric field method has been developed and proven to be effective for preform design problems [3]. However, the equipotential lines cannot be directly used to surrogate the preform contours. As it is difficult to fully automate the design process, considerable manual interventions through CAD software are often required with reduced efficiency. A few other approaches in preform design are based on optimization methods, such as response surface method [4], sensitivity

analysis [5, 6], and genetic algorithm [7]. In using sensitivity analysis, the developed algorithm is programmed into finite element model (FEM) code and the derivation of parameter responses sometimes can only be obtained for a specific objective function, which restricts its application to general preform problems. The evolutionary based on genetic algorithm requires a large number of samples, so this can make the computing cost very high. Another widely used approach for preform design is the inverse simulative method which was firstly proposed by Park et al. [8]. This approach starts from the desired final shape of a forged component and traces back to the state of the previous step by reversing the direction of the velocity field. Based on this approach, the preforms of H-shaped cross-sectional components [9], airfoil section blade [10], and turbine disk [11] are investigated. In addition, Gao et al. [12] designed the preform shape of a 3D airfoil blade sections by using the inverse FEM approach. However, in this approach, the nodal separation criterion is complicated and the accuracy is insufficient for applying to actual forming operations especially for 3D complex problems involving large material deformation.

Another possible approach for preform design is the evolutionary topological approach used in preform design of bulk metal forming process. The conventional topological optimization method is mainly used for structural design such as car body panels [13], aircraft frames [14], and forming tools [15] by optimizing the material layout within given a design space and defined boundary conditions. There are a number of strategies in topology optimizations including solid isotropic microstructure with penalization (SIMP) [16], homogenization method [17], and evolutionary structural optimization (ESO) [18]. Rozvany reviewed the SIMP- and ESO-related optimization methods [19]. He suggested that SIMP is based on rigorous gradient derivation while ESO is fully heuristic and inefficient in computation. Enhancements of ESO were made by developing a bidirectional evolutionary structural optimization approach, i.e., bidirectional evolutionary structural optimization (BESO) [20], using sensitivities [21, 22] and combination of SIMP and BESO [23]. Concerning topology optimization in metal forming applications, Naceur et al. optimized the shape of initial blank in a sheet metal forming process [24]. The authors also developed a preform optimization algorithm which optimized the preform shape of forging problems based on the BESO method [25]. In the algorithm, an element removal and addition criterion based on hydrostatic stress (one third of the first invariant of the stress tensor) is proposed to optimize material distribution in the forging process. However, as mentioned above, forging optimization is a multi-objective task, and some goals such as deformation uniformity, die cavity filling, and forging load reduction may also have to be achieved for improved forging qualities and reduced cost.

Based on the previous work on preform shape optimization using the BESO approach, a strain-based elementary elimination and addition criterion has been proposed in this paper to fulfill these objectives. The results are compared and evaluated by implementation of the BESO method in forging of a blade and a disk. The rest of the paper is organized as follows: the evolutionary optimization method and boundary smoothing algorithm are first presented. Two 2D case problems including forging of an aerofoil shape and a disk are studied with preform design optimization results obtained. This is followed by concluding remarks in the end of the paper.

2 BESO-based forging preform design optimization method

BESO optimization algorithm was mainly developed for light weight design of continuum structures under loading of elastic deformation. In BESO, material can be added and at the same time removed from the structure based on certain criteria with improved computational efficiency. Similarly, the same principle may be used for the preform design optimization in forging applications: unwanted material may be removed while more material may be added in certain regions of the preform in the optimization iterations. During optimization iterations, the preform shape would approach the optimum of the forging properties. For BESO to be applied to metal forming problem, there are a number of technical challenges due to the different features between forging operations and elastic loaded structures:

1. In forging process, the workpiece is required to be continuum without any inside voids. In order to comply with this specific feature, modifications of preform shape in the optimization process can only be implemented on the boundary of the workpiece.
2. Forging simulation involves complex contact conditions, so the intermediate finite element (FE) model with jagged surfaces after element addition and removal operation has to be smoothed to avoid forging defects such as folding.
3. In ESO, the von Mises stress is commonly used as element addition and removal criterion. However, von Mises stress cannot be used to differentiate compressive or tensile condition of the deformed material. Therefore, new robust criterion for element addition or removal has to be developed to optimize the forging uniformity with the premise of sufficient die filling.

In the previous research, the above challenges (1) and (2) were overcome by developing a new BESO algorithm for element filtering and boundary smoothing [25]. However, the element addition and removal criterion has a significant impact on the final preform shape and the computational

efficiency. In-depth investigation on the element addition and removal criteria is necessary for the improved optimization result and efficiency.

2.1 Optimization objective

The basic objective of forging is to achieve a desired preform shape which enables sufficient filling of die cavity and minimization of flash. An advanced forging optimization objective is to increase the deformation uniformity with better mechanical properties, which is especially significant for hot forging products. As illustrated in Fig. 1, the objective for the die filling can be defined by the following equation:

$$\psi = \frac{S_U + S_F}{S_D} \tag{1}$$

where S_D is the die surface (without flash land) representing the desired workpiece shape; S_U and S_F are the surfaces of the unfilled die cavity and the flash, respectively. In actual forging practice, there are always some flash to avoid the unfilled die cavity. So, the actual volume of preform will be slightly larger than that of designed one.

The second objective aims to evaluate the deformation uniformity of forged components, which can be described by:

$$\overline{\varepsilon}_{S.D.} = \sqrt{\frac{\sum_{i=1}^{n} \left(\overline{\varepsilon}_{e,i} - \overline{\varepsilon}_e^a\right)^2}{n-1}} \tag{2}$$

where $\overline{\varepsilon}_{S.D.}$ is standard deviation of the equivalent strain field, $\overline{\varepsilon}_{e,i}$ is the equivalent strain of element i, $\overline{\varepsilon}_e^a$ is the average strain for all elements, and n is the total number of elements.

Considering Eqs. (1) and (2), the measures of the objectives, ψ and $\overline{\varepsilon}_{S.D.}$ are correlated to the forging practice: unfilled die cavity implies that there is no direct compression from the die surface, which implies insufficient material deformation in the die stroke direction. For the material around the contact region, deformation could have occurred. However, it is difficult to optimize the die filling and deformation uniformity simultaneously. In this work, Eq. (1) is employed as the optimization objective to control the optimization iterations: the optimization iteration should be stopped when ψ is reduced to a certain extent. In addition, a maximum iteration number should be specified: if the iteration number is larger than the specified number, the optimization process will be stopped. Equation (2), as an indication of the degree of deformation uniformity, is employed to evaluate the robustness of optimization algorithm.

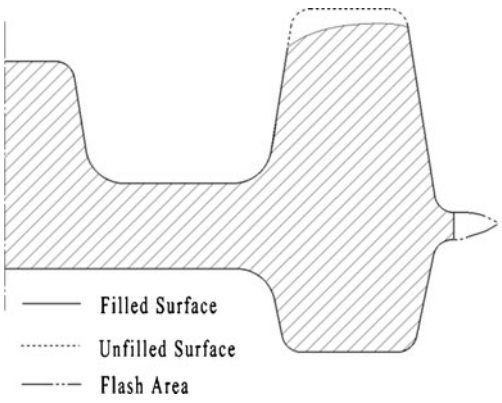

Fig. 1 Definition of surface area

2.2 Optimization strategy

The optimization strategy is illustrated in Fig. 2. Initially, a background mesh is created by using an equally spaced grid. Each element in the background mesh has two states: active or inactive. All active elements during the optimization iteration process constitute the pattern of current preform solid structure. An initial preform shape must be given in advance and used in the first FE simulation. By obtaining forging simulation results, the developed program will automatically calculate and analyze whether the objective function satisfies the specified tolerance: if yes, the optimization program terminates and the current preform shape will be used as the optimized preform shape; otherwise, the optimization process is implemented in the following sequences: (1) Data interpolation operation tracks each element deformation history so that relevant field quantities can be transferred from the forming FE mesh back to the background mesh. (2) Base on the last iterative preform shape, the element addition and removal criterion is implemented and the active and inactive elements are updated to form a new preform shape. (3) As the new boundary after topology optimization is jagged and cannot be directly used for FE simulation, a B-spline surface approximation method is employed to smooth the boundary surface according to the surface node positions of the preform topology model. The approximated shape of the new preform geometry contour is imported into the DEFORM 2D software package, an unstructured mesh can be generated automatically by the FE system, and the workpiece mesh is assembled with die models to form a complete FE model for next forging simulation. The above process repeats until the termination of iteration cycle and the final optimized preform are obtained.

2.3 Strain-based element addition and removal criterion

Concerning the element treatment in topology optimization, in conventional topological optimization for structural design, elements may be removed from the regions which are under stressed and added to the regions of over

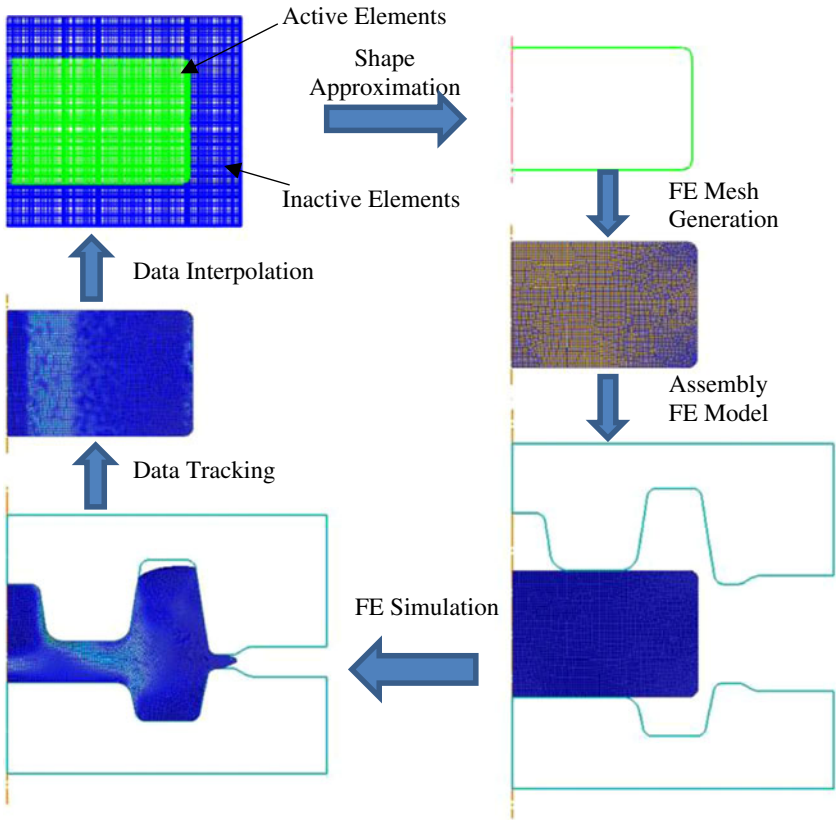

Fig. 2 BESO strategy for preform design

stressing. Similarly in metal forming process, the materials in the vicinity of unfilled die cavity are normally under tensile stress state, and it implies that there are insufficient materials in the regions so elements may be added; whereas for the regions under compressive stress state, it implies that materials may be removed from the regions. Hydrostatic stress other than the von Mises stress has been employed in the criterion to evaluate the final tensile or compressive stress state of forged parts. Hydrostatic stress σ_m is defined by the mean of three principal stresses, which is given by Eq. (3).

$$\sigma_m = \frac{\sigma_1 + \sigma_2 + \sigma_3}{3} \tag{3}$$

where σ_1, σ_2, and σ_3 are the three principal stresses. Hydrostatic stress can effectively evaluate the tensile or compressive state of materials: if $\sigma_m > 0$, the element is under tensile stress state, and if $\sigma_m < 0$, the element is under compressive stress state. This criterion has been proven to be effective in BESO-based preform design optimization [25].

Although hydrostatic stress can effectively be used to reflect the die filling status, it does not correlate to the forging uniformity directly. In the calculation of material deformation, equivalent strain $\overline{\varepsilon}_e$ is generally used to evaluate the overall degree of material deformation. The deformation uniformity can be improved if $\overline{\varepsilon}_e$ of each single element approaching the average value of the all elements. In this way, elements with higher equivalent strain may be decreased by reducing the surround material, while the element with lower equivalent strain may be increased by adding material. However, one problem of using the equivalent strain is that it does not reflect the tensile or compressive deformation state so it cannot be directly used to optimize the die filling. In order to include the deformation state, a single strain component ε_z has been added in the criterion as most of the material deformation is expected to occur in the loading direction in the forging process, i.e., large positive ε_z value indicates tensile strain state in the loading direction, which implies insufficient die filling and more material to be added in the surrounding regions. In contrast, negative ε_z value shows compressive strain state indicating more than enough material for necessary die filling, which implies material to be removed. In this way, the deformation uniformity and die filling can be both considered by including the equivalent strain $\overline{\varepsilon}_e$ and the strain component in the vertical direction ε_z. The criterion of strain uniformity $\overline{\varepsilon}_e^d$ can be expressed by Eq. (4).

$$\overline{\varepsilon}_e^d = u_1 \cdot \frac{\overline{\varepsilon}_e{}^i}{\overline{\varepsilon}_e{}^{\max} - \overline{\varepsilon}_e{}^{\min}} - u_2 \cdot \frac{\varepsilon_z^i}{\varepsilon_z^{\max} - \varepsilon_z^{\min}} \tag{4}$$

Where $\bar{\varepsilon}_e^{\,i}$, ε_z^i are equivalent strain and strain component in the loading direction of element i; $\bar{\varepsilon}_e^{\max}$, $\bar{\varepsilon}_e^{\min}$, $\varepsilon_z^{\max}$, and $\varepsilon_z^{\min}$ are the maximum and minimum value of equivalent strain and vertical strain component of the model, respectively; u_1 and u_2 are weighting coefficients and assigned to be 0.5 in this study. In Eq. (4), the first term $\frac{\bar{\varepsilon}_e^{\,i}}{\bar{\varepsilon}_e^{\max}-\bar{\varepsilon}_e^{\min}}$ is a normalized equivalent strain, which indicates the degree of the overall deformation but not the deformation state; the second term $\frac{\varepsilon_z^i}{\varepsilon_z^{\max}-\varepsilon_z^{\min}}$ is a normalized vertical strain component, which can be considered as a correction of actual deformation state. Large $\bar{\varepsilon}_e^d$ value implies the material in a local region is under large compressive deformation especially in the vertical direction, and the material has to be removed to increase the deformation uniformity; small $\bar{\varepsilon}_e^d$ value implies the local material is under tensile deformation, and additional material is required in the vicinity of the area to increase the compressive material deformation. Using these attributes, the strain-based criterion $\bar{\varepsilon}_e^d$ is employed in the element addition and removal criterion as compared to the hydrostatic stress criterion [25].

In order to decide the total number of background elements to be added (N_{addition}) and removed (N_{removal}), the ratio between N_{addition} and N_{removal} is determined by the actual model volume V_{actual} and the pre-calculated desired model volume V_{target}:

$$\frac{N_{\text{addition}}}{N_{\text{removal}}} = \left(\frac{V_{\text{target}}}{V_{\text{actual}}} - 1\right) \Big/ w_1 + 1 \tag{5}$$

As V_{actual} and V_{target} in Eq. (5) are quite similar in some forging cases in which the workpiece volume is very large but unfilled die cavity is very small, an acceleration factor w_1 is defined to magnify this ratio: $0<w_1\leq 1$. If $V_{\text{actual}}>V_{\text{target}}$, the total number of element volume to activate in the model will be less than the total number to deactivate; otherwise, the total number to activate in the model will be more than the total number to deactivate.

Although Eq. (5) gives the ratio of $N_{\text{addition}}/N_{\text{removal}}$, the actual numbers of elements to activate or deactivate are to be determined. As only surface elements can be activated or deactivated, the sum of N_{addition} and N_{removal} should not be larger than the total number of elements on the outside surface of workpiece N_{surface} and the detailed relationship can be described by:

$$(N_{\text{addition}} + N_{\text{removal}})\cdot w_2 = N_{\text{surface}} \tag{6}$$

Where w_2 is a factor to control the modification speed: $0\leq w_2\leq 1$.

Using Eqs. (5) and (6), the total number of elements to activate N_{addition} and to deactivate N_{removal} can be calculated. In the program, all elements at the boundary surface are sorted according to their field values according to Eqs. (7) and (8), so the critical values ξ_{RR} and ξ_{AR} can be obtained, where ξ_{RR} is the $N_{\text{removal}}^{\text{th}}$ smallest threshold value and ξ_{AR} is the $N_{\text{addition}}^{\text{th}}$ largest threshold value. So, the elements to activate and deactivate can be determined by the following equations:

$$\xi_e \leq \xi_{\text{RR}} \tag{7}$$

$$\xi_e \geq \xi_{\text{AR}} \tag{8}$$

Where ξ_e is the elementary field value before unloading.

2.4 Boundary smoothing and data tracking algorithms

The background mesh contains jagged boundary surface so it cannot be directly used for FE simulation. To smooth the boundary of model, a surface approximation technology is employed based on a standard procedure [26]. Figure 3a shows an example of the approximated surface from the background mesh. Figure 3b shows the generated FE mesh of smooth approximated surface. As can be seen from the figure, the mesh quality is improved compared to the original background mesh. However, this operation may change the volume of workpiece. This problem may be avoided by using more control points for B-spline curve and finer background mesh.

After the FE simulation, relevant field values from simulation result database need to be transferred from the forged FE

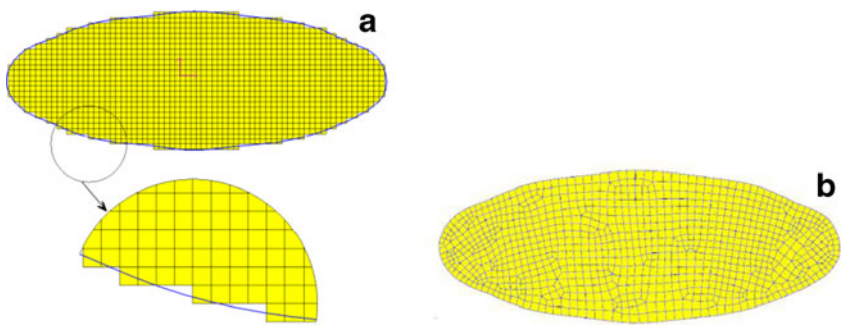

Fig. 3 **a**, **b** Smoothing of boundary from background mesh

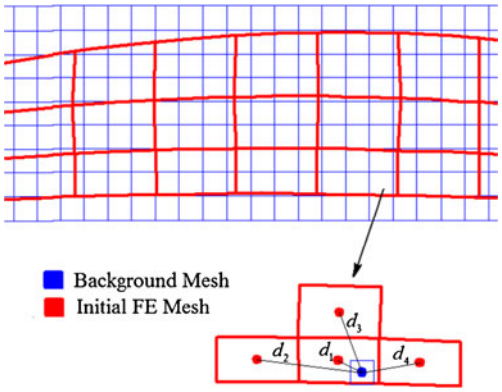

Fig. 4 Data transformation step from initial FE mesh to background mesh

mesh back to the structured background mesh for element removal and addition operation. During the forming process, severe plastic deformation of the workpiece model may cause distortion in the initial FE mesh and trigger the remeshing operation. So, the first step is a data tracking process from the remeshed final FE mesh to the initial FE mesh. The detailed description may be referred to the literature [25]. If no remeshing operation is required during the forming process, the first step may be ignored. The second step is to interpolate data from the initial FE mesh into the background mesh. The two meshes should be placed in the same coordinate system. In this step, the state variables ξ_i at integration point (blue point in Fig. 4) for each element in the background mesh are inversely weighted by their distances d_i to a patch of n integration points (red points in Fig. 4) from the initial FE mesh. The interpolation function is given in Eq. (9).

$$\xi = \left(\sum_{i=1}^{n} \frac{\xi_i}{d_i^2}\right) \cdot \left(\sum_{i=1}^{n} \frac{1}{d_i^2}\right)^{-1} \tag{9}$$

Using the above steps, the state variables obtained through FE simulation results can be assigned to each background element for following element removal and addition operation.

2.5 Shape complexity

The proposed optimization algorithm may be used to improve the deformation uniformity in forging processes. Other than the deformation uniformity, the shape complexity of the preform is another factor that affects the forging difficulty. Different methods have been developed to evaluate the shape complexity [27, 28]. In this work, the shape complexity value C is calculated by the ratio between the volume of the forged part and the volume of the circumscribing over the forging figure. For a 2D forging problem, the shape complexity index C can be calculated by:

$$C = S_f / S_c \tag{10}$$

where S_f is the area of forging and S_c is the circumscribing area of forging profile. Considering the shape complexity definition, the bigger the C value is, the simpler the preform and forging shape will be. Using this C value, the shape complexity of each forging model can be evaluated.

2.6 Optimization system

The flowchart of the optimization system is shown in Fig. 5. The modifications of elements are within a predefined background mesh. An initial workpiece shape is defined and FE analysis is carried out. After each FE simulation, the final workpiece shape is checked. If the performance index is out of the tolerance (for example: ψ=0.05 is defined in the case of forging of an aerofoil section, which means that surfaces at the flash and unfilled die cavity area should be less than 5 % of the effective die surface), the relevant field values are tracked and

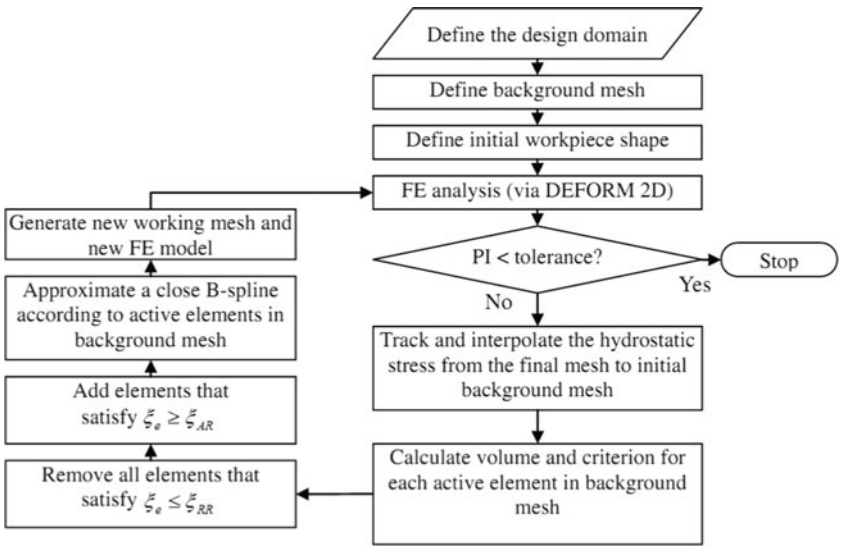

Fig. 5 Flowchart of topology optimization process

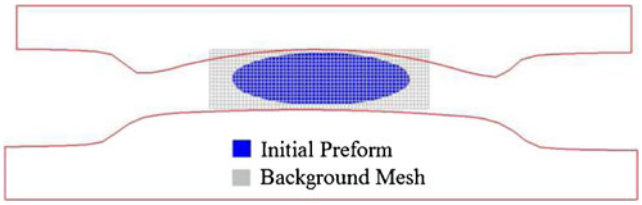

Fig. 6 Definition of background mesh, initial preform, and FE model

interpolated for each active element in the background mesh. Then, element activation and deactivation are implemented for all elements in the background mesh based on the developed topological optimization method and constraints. Therefore, a new preform shape is obtained by extracting all the active elements on the boundary from the background mesh and a B-spline curve is approximated. According to the shape of the B-spline curve, a new mesh of the preform shape is generated and the FE model is updated. Then, FE simulation is run again with the above computational steps repeated until the objective function reaches the specified tolerance. The automation of the topological preform design optimization is achieved by using a developed program written in C# code. The element removal and addition in the background mesh, B-spline surface approximation, data extraction from DEFORM 2D database, and data transformation are implemented by using this in-house program. This program also calls the DEFORM 2D software package for FE forging simulation and FE mesh generation in the background.

3 Case studies

3.1 Forging of an aerofoil section

In the FE simulation, INC718 material is employed referring to the literature [29]. Workpiece is defined to be rigid-viscoplastic and the FE model is subdivided into quadrilateral isoparametric mesh, while the forging dies are set as rigid body in the forging process simulation. An elliptical shape which has a volume of approximately 119 % of the theoretical forging volume is adopted as the initial shape of billet. The iterative process finishes when the forged preform volume is reduced to less than 105 % of the theoretical forging volume (ψ=0.05). The definition of the FE model is shown in Fig. 6.

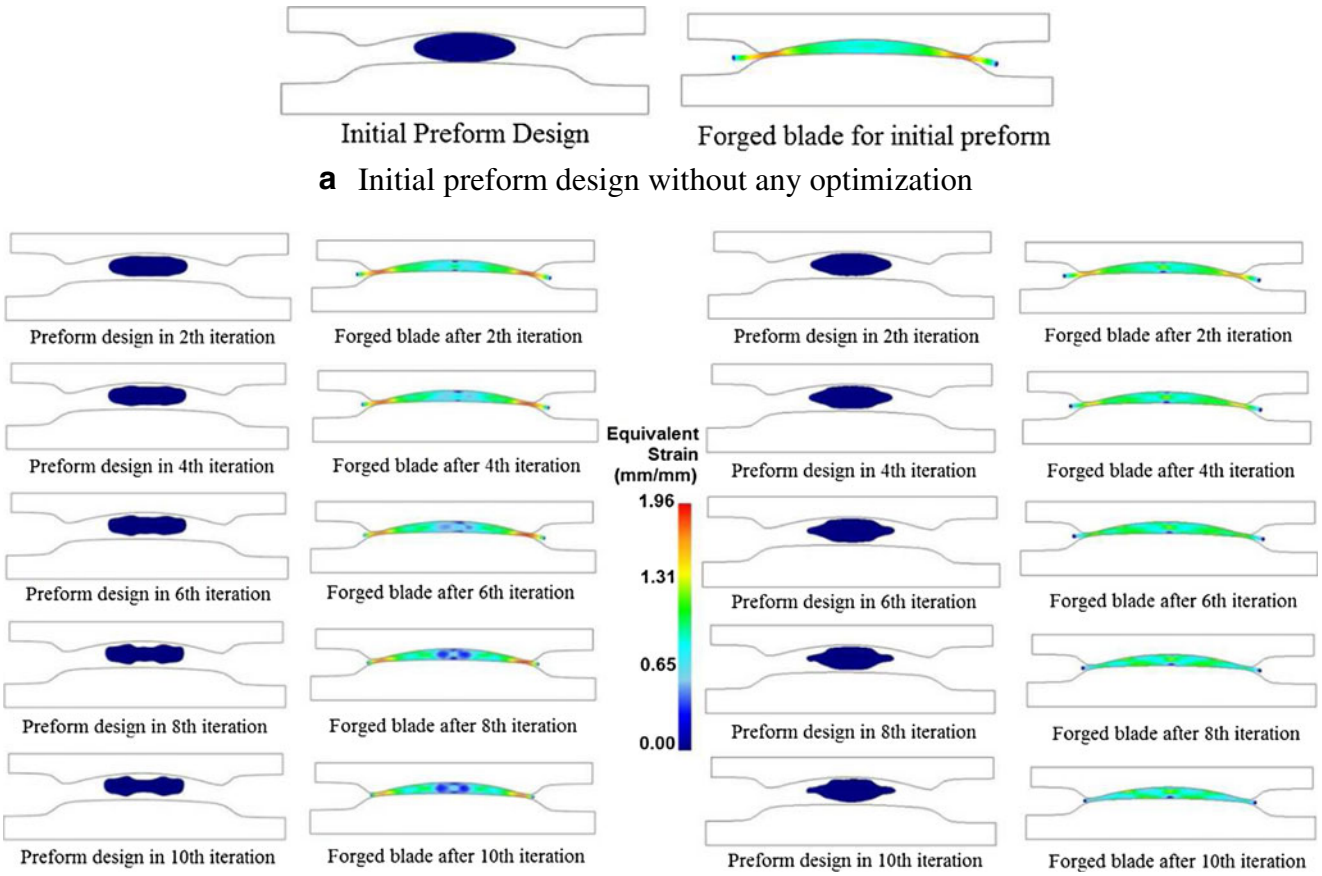

a Initial preform design without any optimization

b Hydrostatic stress as element removal and addition criteria

c Strain uniformity as element removal and addition criteria

Fig. 7 Evolutionary process for different optimized preform and corresponding equivalent strain distributions

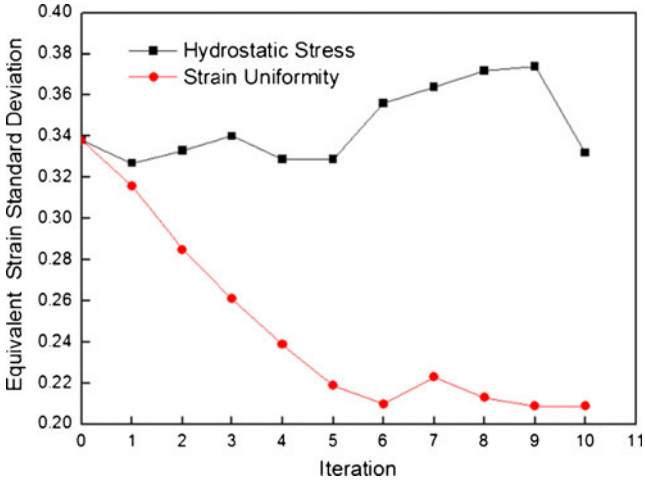

Fig. 8 Numerical analysis of equivalent strain standard deviation $\bar{\varepsilon}_{S.D.}$ for forged blades after 10th iteration

The background mesh consists of 15,296 grids. The initial forging temperature of workpiece is 1,010 °C and the die temperature is 250 °C. The friction factor between the workpiece and the die is 0.3. The upper die velocity is 200 mm/s and the low die is stationary in the forging process simulation. Detailed flow stresses of the work material as a function of strain, strain rate, and temperature can be obtained in the literature [29].

Figure 7 shows the FE simulation results of the preform shape evolution and the corresponding equivalent strain distributions of different element removal and addition criteria. As can be seen in the figure, different preform shapes have been obtained by using the two algorithms. The complexity of the optimized shapes is acceptable, which can be made by forging or extrusion process. Concerning the material flow, for initial preform model, excessive equivalent strain exists at the two ends of the flash area of the aerofoil section where more than enough material leads to intensely flow deformation (Fig. 7a). In both preform cases, the flash area of the forged

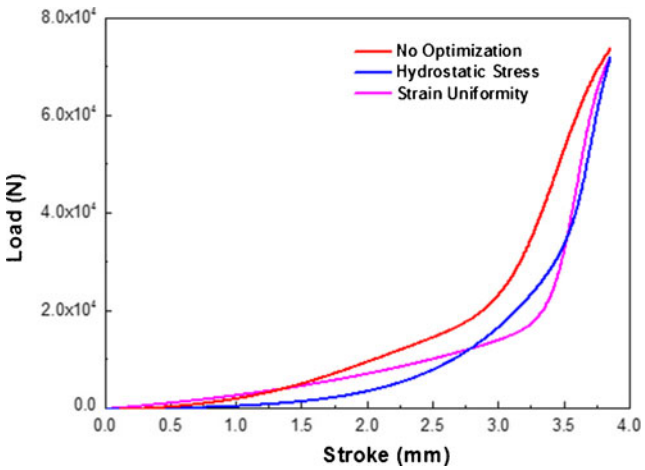

Fig. 9 Comparison of load–stroke curve between different preform situations

Table 1 Comparison of shape complexity

Model	Final forging part	Initial preform with no optimization	Preform with hydrostatic stress optimization	Preform with strain uniformity optimization
C	0.48	0.80	0.76	0.64

blade dropped gradually with reduced equivalent strain. However, larger equivalent strain can be observed in the flash area by using the stress-based criterion than that of the strain-based criterion. These results suggest that the optimized preform shape obtained from the strain-based criterion is superior in reducing the high strain values in local area. This shows that better deformation uniformity can be achieved effectively during forging process.

Figure 8 compares the deformation uniformity $\bar{\varepsilon}_{S.D.}$ described in Eq. (2) by using the stress-based and strain-based criteria. It can be found that the strain standard deviation results $\bar{\varepsilon}_{S.D.}$ decrease constantly from the strain-based optimization, but this is not the case in the stress-based optimization. The final values of $\bar{\varepsilon}_{S.D.}$ are about 0.332 and 0.209 after 10 iterations, respectively, from an initial value of about 0.338 for both cases, which suggests a reduction of 2 and 29 %, respectively. This result is consistent with the observation given in Fig. 7, in which the strain-based criterion is more effective in achieving improved material deformation uniformity.

Figure 9 compares the load–stroke curves from the preform shape after 10th optimization iterations by different element removal and addition criteria and forged preform without any optimization. For the optimized

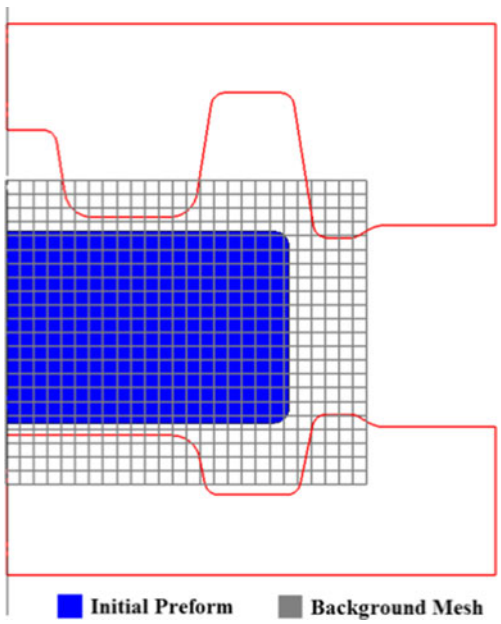

Fig. 10 Definition of background mesh, initial preform, and FE model

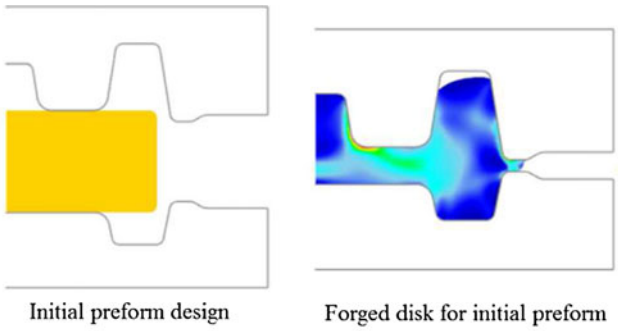

a Initial preform design without any optimization

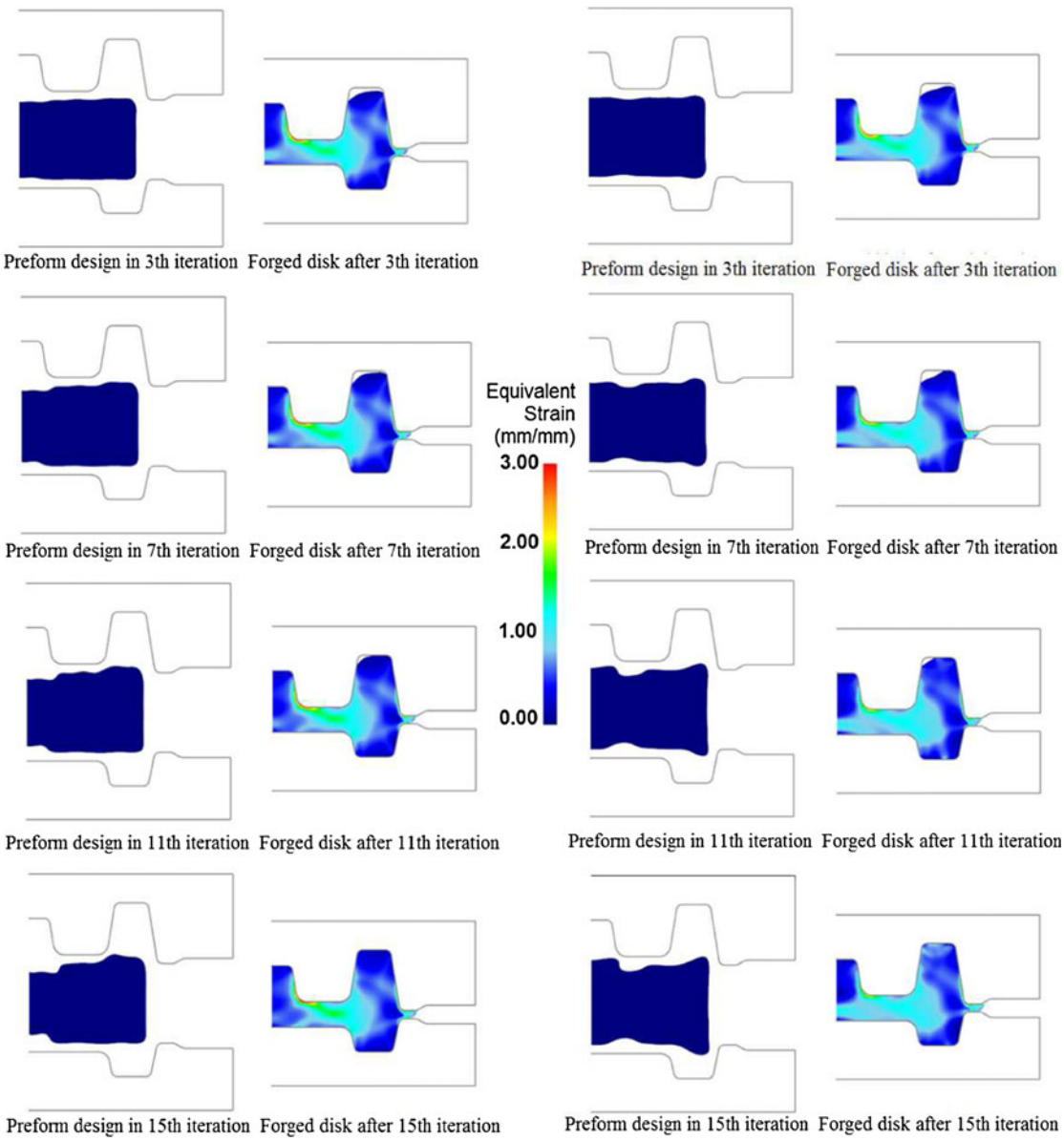

b Hydrostatic stress as element removal and addition criteria

c Strain uniformity as element removal and addition criteria

Fig. 11 **a**–**c** Evolutionary process for different optimized preforms and corresponding equivalent strain distributions

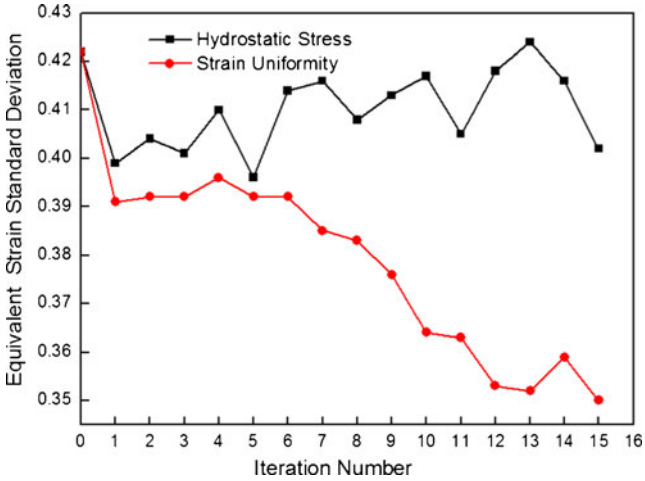

Fig. 12 Changes of equivalent strain standard deviation $\bar{\varepsilon}_{S.D.}$ in evolution iterations

preforms, the forging loads during the total forming process are about 5 % lower than the preforming process without optimization. It suggests that the optimized preforms combined with improved material volume result in better material flow and reduced deformation resistance during the forming process. Comparing with the two optimized preforms, the forging load increased quickly from the strain-based criterion at the initial stage. However, almost the same maximum load on the two optimized curves indicates that the final forged shapes are very close and the two preforms have the same amount of volume.

Concerning the shape complexity of the forging shape before and after optimization, Table 1 shows the C values for all the forging models. As can be seen in the table, the shape complexity of the preforms increases as compared to the initial preform shape without optimization. Comparing the preform shapes, the shape obtained by strain uniformity

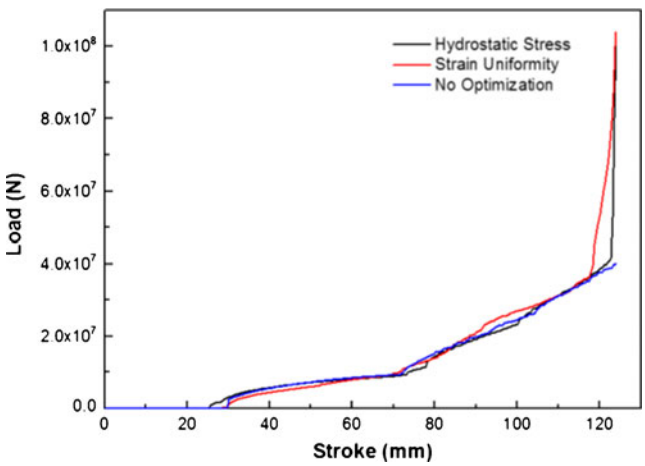

Fig. 13 Comparison of load–stroke curve between different preforms situation

Table 2 Comparison of shape complexity

Model	Final forging part	Initial preform with no optimization	Preform with hydrostatic stress optimization	Preform with strain uniformity optimization
C	0.54	1	0.87	0.85

criterion is more complex than that by the hydrostatic stress criterion. This result suggested that the improvement of forging uniformity brings a more complex shape of preform in a certain extent. However, the shape complexity of preform is still better than the final forged part, which suggests that the shape of preform is acceptable.

3.2 Forging of an axisymmetric plane of a disk

Disk forming is another typical application of hot forging. In the FE model, AISI-1050 steel material is employed from DEFORM material library. A rectangle shape of axisymmetric model is adopted as the initial shape of billet. The iterative computation stops when the forged preform achieves sufficient die filling. The definition of the FE model is shown in Fig. 10. The background mesh consists of 61,104 grids. The initial forging temperature of the workpiece is 1,120 °C and the die temperature is 300 °C. The friction factor between the workpiece and the die is 0.3. The upper die velocity is 100 mm/s and the low die is stationary in forging simulation. Other simulation parameters are the same as to the case of the forging of aerofoil section.

Figure 11 shows the FE simulation of the preform shape evolution and the corresponding strain distributions using both the stress-based and strain-based criteria. As shown in Fig. 12a, insufficient die filling can be observed from the initial preform, which indicates the inappropriate forging design when the flash of the forged disk is formed at the end of forging process. The difference of two element addition and removal criteria results in quite different optimized shapes. In the optimization process for both cases, the die filling improved continuously with the evolution of preform shapes and satisfactory die filling can be achieved after the 15 iterations. By comparing the strain distributions, it can be found that the preform optimized by using the strain-based criterion gives better performance in avoiding the local high strain concentration than that by using the stress-based approach as shown in Fig. 11b, c.

Figure 12 shows the changes of deformation uniformity described by the strain standard deviation for models using different criteria. Similar results can be observed: the $\bar{\varepsilon}_{S.D.}$ value reduces more quickly in the strain-based optimization, while in stress-based optimization, the $\bar{\varepsilon}_{S.D.}$ value oscillates during the optimization

process. With an initial value of 0.422, the $\overline{\varepsilon}_{S.D.}$ dropped to 0.35 with a reduction rate of 18 % in strain-based optimization after 15th iterations, which suggests that the strain-based approach can improve the deformation uniformity more effectively in the forging process.

Figure 13 compares the load–stroke curves from the forged preforms at 15th optimization iteration by different element removal and addition criteria and the forged preform without any optimization. As can be seen in the figure, the maximum forging load for the preform without optimization is much lower than that for the optimized preforms. This is because of the insufficient die filling from the initial preform. As there is little difference in the flash region for both optimized preforms as shown in Fig. 11b, c, almost the same forging load is required in using both stress-based and strain-based approaches.

The comparison of shape complexity of the models is given in Table 2. Similar results are obtained: the optimized preforms are more complex than the initial preform shape and the shape complexity obtained by the strain uniformity criterion is slightly higher than that optimized by the hydrostatic stress criterion. The shape complexity of preform is much better than the final forging part, which suggests that the shape of preform is satisfactory.

4 Discussion and conclusion

Bulk metal forming is a process to deform the shape of billet to achieve the designed part geometry. The preform design, as a middle stage between the initial billet and the final forged part, is often necessary to optimize the material flow, avoid defect, and improve the material performance. Obtaining an optimized preform with a proper volume and a precise shape is always a challenge. In this paper, a strain-based element removal and addition criterion has been introduced in the BESO-based shape optimization process for bulk metal forming applications. In this criterion, two specific considerations are given, i.e., the degree of material deformation and the state of either tension or compression of material deformation in the forging process. By combining these two factors, the rules to determine the element removal and addition can be easily defined: surface material with excessive compressive deformation is removed from the preform and the material is added around the surface point under large tensile deformation.

Two forging cases are employed to evaluate the robustness of this newly developed strain-based approach by comparing with the stress-based approach. Started from an initial preform with either larger or smaller volume, both optimization algorithms worked well in die cavity filling. Thus, the basic objective of forging can be achieved. In consideration of deformation uniformity, better material flow can be obtained with the strain-based criterion as the value of $\overline{\varepsilon}_{S.D.}$ described by Eq. (2) can obviously be reduced. This result suggests that the strain-based criterion shows better performance in forging deformation uniformity and simpler outline shapes at the same time.

Following conclusions may be drawn from this work:

1. BESO-based approach is proven to be effective in shape optimization of metal forming problems with involvement larger material deformation.
2. The newly developed strain-based criterion has shown obvious advantages over the stress-based criterion in improving the material deformation uniformity.
3. The complexity of the optimized shape is acceptable, which is possible to be made by forming or extrusion using specifically designed tools and dies.
4. The BESO-based preform optimization using the strain-based criterion is computationally efficient as only 10–20 iterations are required for both case studies. This is a particularly attractive feature for the time-consuming forging simulations.

Acknowledgments The research is supported by the National Nature Science Foundation of China 51005150.

References

1. Sheu J, Yu C (2009) Preform and forging process designs based on geometrical features using 2D and 3D FEM simulations. Int J Adv Manuf Technol 44:244–254
2. Lee SR, Lee YK, Park CH, Yang DY (2002) A new method of preform design in hot forging by using electric field theory. Int J Mech Sci 44:773–792
3. Cai J, Li FG, Liu TY (2011) A new approach of preform design based on 3D electrostatic field simulation and geometric transformation. Int J Adv Manuf Technol 56:579–588
4. Yang YH, Liu D, He ZY, Luo ZJ (2009) Multi-objective preform optimization using RSM. Rare Metal Mater Eng 38:1019–1024
5. Zhao G, Ma X, Zhao X, Grandhi RV (2004) Studies on optimization of metal forming processes using sensitivity analysis methods. J Mater Process Technol 147:217–228
6. Zhao X, Zhao G, Wang G, Wang T (2002) Preform die shape design for uniformity of deformation in forging based on preform sensitivity analysis. J Mater Process Technol 128:25–32
7. Roy S, Ghosh S, Shivpuri R (1997) A new approach to optimal design of multi-stage metal forming processes with micro genetic algorithms. Int J Mach Tools Manuf 37:29–44
8. Park JJ, Rebelo N, Kobayashi S (1983) A new approach to preform design in metal forming with the finite element method. Int J Mach Tool Des Res 23:71–79
9. Kim N, Kobayashi S (1990) Preform design in H-shaped cross sectional axisymmetric forging by the finite element method. Int J Mach Tools Manuf 30:243–268
10. Kang BS, Kim N, Kobayashi S (1990) Computer-aided preform design in forging of an airfoil section blade. Int J Mach Tools Manuf 30:43–52

11. Zhao G, Zhao Z, Wang T, Grandhi RV (1998) Preform design of a generic turbine disk forging process. J Mater Process Technol 84: 193–201
12. Gao T, Yang H, Liu Y (2006) Backward tracing simulation of precision forging process for blade based on 3D FEM. Trans Nonferrous Metals Soc China 16:639–644
13. Xu Z, Lin Z, Wang H (2006) Lightweight design of auto-body structure by topology optimisation based on level set method. IET Conf Publ 2006:1818–1823
14. Deng Y, Chen H, Ma M, Zhang Y (2005) Studies of aircraft frame design based on topology optimization. Struct Environ Eng 32:39–45
15. Anna N, Frida B (2007) Topology optimization of a stamping die. AIP Conf Proc 908:449–454
16. Rozvany G, Zhou M, Birker T (1992) Generalized shape optimization without homogenization. Struct Multidiscip Optim 4:250–252
17. Suzuki K, Kikuchi N (1991) A homogenization method for shape and topology optimization method. Comput Methods Appl Mech Eng 93:291–318
18. Xie YM, Steven GP (1993) A simple evolutionary procedure for structural optimization. Comput Struct 49:885–896
19. Rozvany G (2009) A critical review of established methods of structural topology optimization. Struct Multidiscip Optim 37:217–237
20. Querin O, Steven G, Xie Y (1998) Evolutionary structural optimization (ESO) using a bidirectional algorithm. Eng Comput 15:1031–1048
21. Huang X, Xie ZM (2008) Topology optimization of nonlinear structures under displacement loading. Eng Struct 30:2057–2068
22. Zhou M, Rozvany G (2001) On the validity of ESO type methods in topology optimization. Struct Multidiscip Optim 21:80–83
23. Huang X, Zuo ZH, Xie YM (2010) Evolutionary topological optimization of vibrating continuum structures for natural frequencies. Comput Struct 88:357–364
24. Naceur H, Guo YQ, Batoz JL (2004) Blank optimization in sheet metal forming using an evolutionary algorithm. J Mater Process Technol 151:183–191
25. Lu B, Ou H, Cui ZS (2011) Shape optimisation of preform design for precision close-die forging. Struct Multidiscip Optim 44:785–796
26. Piegl L, Tiller W (1997) The NURBS book, 2nd edn. Springer, Berlin
27. Zhao G, Wright E, Grandhi RV (1995) Forging preform design with shape complexity control in simulating backward deformation. Int J Mach Tools Manuf 35:1225–1239
28. Tomov B, Radev R (1997) Shape complexity factor for closed die forging. Int J Mater Form 3:319–322
29. Lu B, Ou H, Armstrong CG, Rennie A (2009) 3D die shape optimisation for net-shape forging of aerofoil blades. Mater Des 30:2490–2500